Biotribology 19 (2019) 100098

Contents lists available at ScienceDirect

Biotribology

journal homepage: www.elsevier.com/locate/biotri

Effect of Synovial Fluid Pressurization on the Biphasic Lubrication Property of Articular Cartilage

Shoko Horibata, Seido Yarimitsu, Hiromichi Fujie*

Graduate School of System Design, Tokyo Metropolitan University, 1-1 Minami-Osawa, Hachioji-Shi, Tokyo 192-0397, Japan

ARTICLE INFO

Keywords:
Squeeze-film effect
Biphasic lubrication
Interstitial fluid
Hydrodynamic pressure

ABSTRACT

The wedge-film and squeeze-film effects have been evaluated as a mechanism of hydrodynamic lubrication without considering the relationship to the interstitial pressurization in biphasic lubrication. We hypothesized that the synovial fluid pressure generated by articular motion suppresses the exudation of the interstitial fluid, enhancing the biphasic lubrication ability of articular cartilage. To verify this hypothesis, the effect of the synovial fluid pressure generated by the wedge-film effect was investigated, and in our previous study, it was found that the synovial fluid plays an important role in hydrodynamic lubrication and biphasic lubrication. In this study, the effect of fluid pressurization generated by the squeeze-film effect on biphasic lubrication was evaluated. First, we measured the pressure distribution in the squeeze-film fluid sandwiched between a plate and an approaching cylindrical polyurethane indenter. Second, a synovial fluid pressure (SFP) articular cartilage model was created in Abaqus based on our previous study, where the exudation of the interstitial fluid from articular cartilage was regulated depending on the pressure difference between the interior and exterior of the cartilage. Third, the fluid load support in the cartilage model was analysed at contact. The results revealed that the squeeze-film pressure increased with increasing approach speed. The fluid load support ratio of the SFP model was higher than that of the standard model at approach speeds of 1, 5 and 10 mm/s. The synovial fluid pressure, induced by the squeeze-film effect, influences the biphasic lubrication property of articular cartilage.

1. Introduction

Articular cartilage is composed of a collagen fibre network, proteoglycans, and a large amount of interstitial fluid and has excellent mechanical properties, such as low friction, high load-carrying capacity, etc. The surface of articular cartilage is lubricated by synovial fluid, which is a viscous solution containing mucopolysaccharides, proteins, and lipids. Synovial fluid plays an important role in the lubrication mechanism of articular cartilage. Many traditional lubrication theories, such as boundary lubrication [1,2], hydrodynamic lubrication [3–5], mixed lubrication [6], etc., have been developed to explain the lubrication mechanism of articular cartilage. In these mechanisms, biphasic lubrication [7,8] is involved in cartilage lubrication at high loads and low friction speed. This theory was based on the framework of the biphasic theory developed by Mow et al. [9], which models cartilage as a biphasic material composed of solid and fluid phases, and both phases resist externally applied compressive loads. In this theory, the frictional resistance remains low owing to the nearly negligible shear resistance of the fluid phase when the fluid phase supports a majority of the externally applied load. Caligaris and Ateshian [10] experimentally ascertained that interstitial fluid pressurization is responsible for reducing the friction coefficient of articular cartilage under the condition designed to mirror physiological conditions.

Previous studies related to biphasic lubrication [11–15] have focused on the effects of interstitial fluid on the lubrication property of articular cartilage. However, the synovial fluid exterior of the cartilage may affect hydrodynamic lubrication and biphasic lubrication, because fluid inflow and outflow occurs at the cartilage surface owing to the pressure gradient between the cartilage and synovial fluid. Hou et al. [16] and Jin et al. [17] analytically determined the effect of the porosity of the articular cartilage on the squeeze-film effect, and they indicated a possibility of inflow of fluid to the cartilage surface. Additionally, Moore et al. and Graham et al. indicated that interstitial fluid in articular cartilage was recovered by inflow of water from the contact periphery, which, in turn, resulted in supporting cartilage lubrication [18–20]. These fluid movements could affect the biphasic lubrication property of articular cartilage. For hydrodynamic lubrication of articular cartilage, the synovial fluid pressure is generated by the squeeze-film and wedge-film effects at a narrow fluid gap between the sliding and approaching cartilage surfaces. Under physiological conditions,

* Corresponding author.
E-mail address: fujie@tmu.ac.jp (H. Fujie).

https://doi.org/10.1016/j.biotri.2019.100098
Received 16 November 2018; Received in revised form 11 February 2019; Accepted 8 May 2019
Available online 11 May 2019

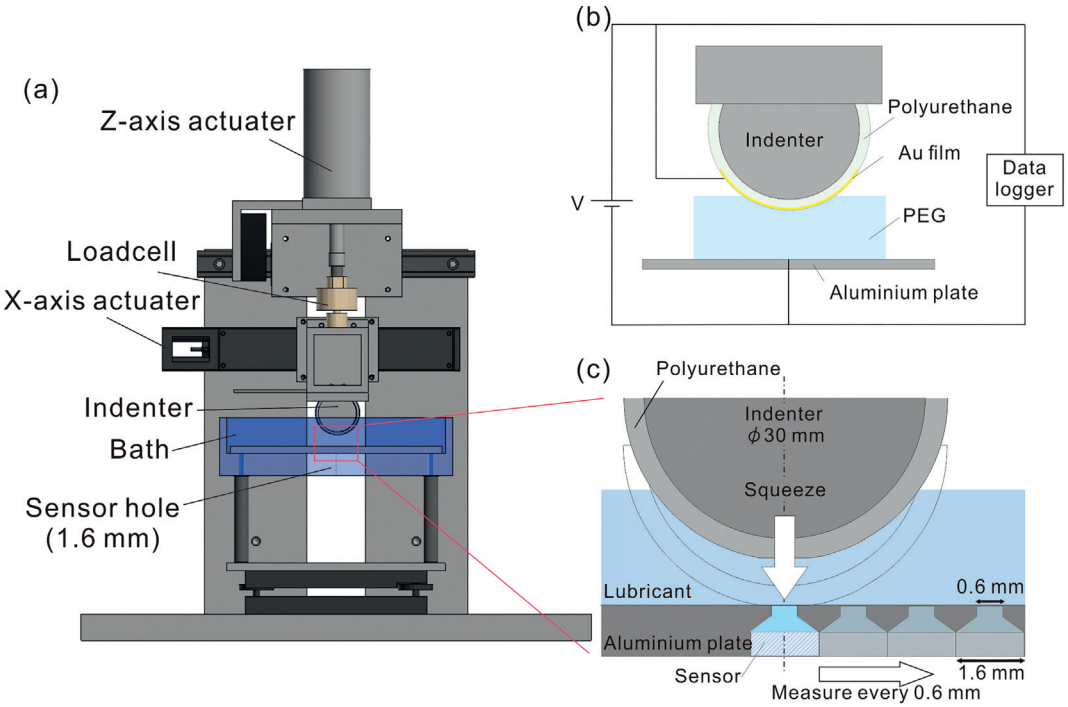

Fig. 1. Experimental apparatus for the measurement of the fluid pressure distribution (a), the electric circuit to detect contact (b), and the experimental scheme (c).

such as walking, the squeeze-film effect plays a more important role than that of the wedge-film effect for hydrodynamic lubrication, owing to the cyclic loading pattern and low sliding speed of articular motion [6,21]. Therefore, in previous studies, the effect of the synovial fluid pressure on the biphasic lubrication property of articular cartilage was evaluated [22–24], and the biphasic lubrication property was enhanced by the wedge-film effect. Therefore, in this study, we performed an experimental and analytical study to determine the influence of the synovial fluid pressure induced by the squeeze-film effect on the biphasic lubrication property of articular cartilage using a poroelastic model.

2. Material and Methods

2.1. Measurement of the Fluid Pressure Distribution

The fluid pressure generated by squeezing was measured using a custom tester (Fig. 1a). A cylindrical aluminium indenter (ϕ = 26 mm) covered with a polyurethane sheet (thickness = 2 mm) was attached to a vertical linear actuator (LAH-46-3002-F, Harmonic drive systems Inc., Japan) with a load cell (LUR-A-500NSA1, Kyowa Electronic Instruments Co., Ltd., Japan). Polyurethane was used as the articular cartilage model material. A flat aluminium plate (A5052, arithmetic average roughness Ra ≤ 11 nm) was attached to the bottom of a liquid bath filled with polyethylene glycol with a viscosity of 0.1 Pa·s (PEG400, FUJIFILM Wako Pure Chemical Corporation, Japan). The viscosity of the polyethylene glycol was selected based on the viscosity of synovial fluid reported by Murakami et al. [25]. A pressure sensor (FOP-M, FISO Technologies Inc., Canada) was embedded in the centre of the aluminium plate. Using this set-up, the polyurethane indenter was approached to contact the aluminium plate with the constant approach speed, and then the applied normal force was controlled until the contact pressure reached to 0.26 MPa. The squeeze film pressure generated in the gap between the indenter and plate was measured with the pressure sensor embedded in the plate. The sampling frequency of the measurement unit for the pressure sensor was 1 kHz. The above-mentioned test was performed at room temperature.

To measure the squeeze-film pressure, the moment of direct contact between the upper indenter and lower plate was required. Therefore, an electric circuit (Fig. 1b) was developed. An Au film was deposited on the polyurethane to provide electrical conductivity using a sputtering device (Quick coater SC-701, ANYU Electron Co., Ltd., Japan). The thickness of the film was approximately 200 nm. Polyethylene glycol used as a lubricant has a high electrical resistivity. Therefore, a change in the applied voltage to the electrical circuit could be detected to verify direct contact between the conductive indenter and plate.

The fluid pressure distribution (Fig. 1c) was measured as follows. First, the centre of the indenter and the pin hole for the pressure sensor were adjusted. Then, the indenter descended from 20 mm above the lower plate until the normal force of 40 N was reached (average contact pressure = 0.26 MPa). The approach speed was 1, 5, or 10 mm/s. Simultaneously, the temporal change of the fluid pressure and voltage were measured to detect direct contact. Then, the indenter position was laterally shifted by 0.6 mm, which is the length of the sensor hole, and the above-mentioned experiment was performed. This procedure was repeated until the distance between the centre of the indenter and sensor hole reached 3.6 mm. We extracted the maximum squeeze-film pressure at the time of direct contact in each measurement position, and we obtained the squeeze-film pressure distribution.

2.2. Construction of FEM Model

A two-dimensional poroelastic cartilage model was developed in Abaqus 6.14 (Dassault Systemes, FR) (Fig. 2). The model contained a 2-mm thick cylinder with an outer diameter of 30 mm consisting of poroelastic elements. Each element was 0.5 × 0.5 mm^2 in size, consisting of a pore pressure, plane strain element (CPE4RP) as an isotropic model of the solid phase of cartilage. This cylindrical cartilage model was fixed on an impermeable and rigid body, and the outflow of water was permitted only at the surface, except for the contact area and lateral cross-section of the cartilage model.

The material properties of the cartilage model are listed in Table 1. The Poisson's ratio of the solid phase was set at 0.49 based on Beatty and Stalnaker [26]. The coefficient of friction of the cartilage to a metal plate in solid-to-solid contact was obtained from our previous study [27]. In the previous study, both a friction experiment and a friction

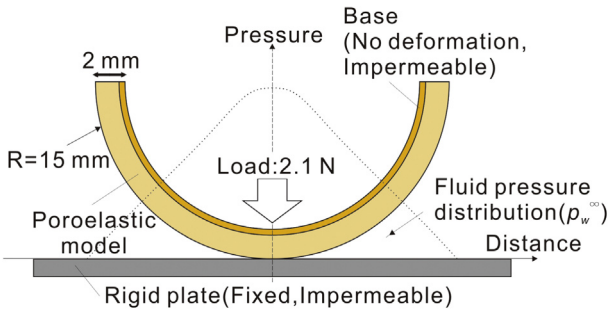

Fig. 2. Compression analysis model with the boundary condition of the fluid pressure.

Table 1
Mechanical properties of the cartilage model.

Solid phase				
Modulus (MPa)	Poisson's ratio	Permeability (10^{-15} m^4/Ns)		Friction coefficient (solid-to-solid contact)
		$k = k_0 exp(M\varepsilon_m)$ [28]		
E_m	ν	k_0	M	μ_b
0.44	0.49 [Ref. 26]	5.55 [Ref. 29]	2.64 [Ref. 30]	0.42 [Ref. 27]

analysis of articular cartilage were performed in a condition where interstitial fluid sufficiently exuded. The coefficient of friction of the cartilage in solid-to-solid contact in the analysis, when the experimental data mostly agreed with analytical data, was adopted in this study. Based on Eq. (1) by Lai and Mow [28], permeability k was formulated with the initial permeability under no strain k_o, permeability coefficients M, and volumetric strain ε. The initial permeability k_0 and permeability coefficient M were determined from our previous studies [29,30].

$$k = k_0 exp(M\varepsilon) \tag{1}$$

For the Abaqus calculation, the strain was transformed to porosity e using Eq. (2)

$$\varepsilon = (e - e_0)/(1 + e_0), \tag{2}$$

where e_0 represents the initial void ratio, defined as the void ratio under no strain. The parameter e_0 was set to 4 because the water content in articular cartilage is approximately 80%, and water is incompressible. In the analyses, Eqs. (1) and (2) were used to determine the permeability in the articular cartilage. The modulus of the solid phase of the cartilage model was determined from a compression test of polyurethane. Cylindrical plug-specimens of polyurethane, 3 mm in diameter and 1.3 mm in depth were extracted from a polyurethane sheet. In the compression test, the specimen was subjected to compressive strain of 10% using a flat impermeable titanium alloy plate. The compressive strain was kept for 30 s for allowing stress-relaxation. Through this test, we obtained a stress-relaxation curve and found that the modulus of polyurethane was 0.44 ± 0.01 MPa (mean ± SE). The obtained properties were applied to the standard articular cartilage model.

To determine the effect of the synovial fluid pressure on the biphasic lubrication property of articular cartilage, a synovial fluid pressure model (SFP model) was established, in which the exudation of the interstitial fluid from the articular cartilage was regulated depending on the pressure difference between the applied fluid pressure and analysed pressure of the surface elements using Eq. (3)

$$v_n = k_s (p_w - p_w^\infty), \tag{3}$$

where v_n, k_s, p_w, and p_w^∞ represent the normal vector of the pore water flow velocity, permeability of the cartilage surface, pore pressure of the surface element, and the synovial fluid pressure, respectively. The synovial pressure distribution data, determined from the fluid pressure distribution from the experiment described in Section 2.1, were plotted against the distance from the centre of the contact area (Fig. 2, dotted line). The pressure data at each measurement position within 3.6 mm were imported into the model as the synovial fluid pressure p_w^∞ of the boundary condition. Although the fluid pressure induced by the squeeze-film effect originally changes with time as the gap decreases, we assumed that it was time-independent and had a spatial distribution, because the period of contact was short. In the standard model, the boundary condition identical to the SFP model was set, except p_w^∞ was zero.

2.3. Compression Analysis

Using the developed articular cartilage models, a compression analysis was performed. The cartilage indenter was used to indent to the rigid surface until the normal force of 2.1 N (average contact pressure = 0.26 MPa) was reached, and the approach speed was 1, 5, or 10 mm/s. The fluid load support ratio was calculated from the integral of the pore pressure p_w at the contact area S divided by the contact force W using Eq. (4).

$$\text{fluid load support ratio} = \int p_w dS/W \tag{4}$$

3. Results

The typical temporal change of the fluid pressure during the squeeze motion is shown in Fig. 3. Two pressure peaks were observed for each measurement in the section from 0 mm to 2.4 mm. Because the squeeze-effect occurred before contact (Fig. 3a, dotted line), the first peak was considered as the squeeze-effect induced peak pressure. Therefore, the pressure at the moment of contact was extracted from the temporal changes of the measured fluid pressure at each approach speed, and the plots are shown in Fig. 3(b–d). For the contact region (0–2.4 mm), there was an increasing squeeze-film pressure with an increasing approach speed. Outside the contact region (2.4–3.6 mm), the pressure decreased as the measurement point diverged from the centre of the indenter.

Then, the obtained pressure distribution at each approach speed was substituted into the SFP model. The fluid load support ratios at 0.1 MPa and 0.26 MPa of a contact pressure were analysed, as shown in Fig. 4. In the standard model, the fluid load support ratio was 67.2%, 69.4%, and 71.7% at 0.1 MPa of a contact pressure and 63.6%, 66.4%, and 67.1% at 0.26 MPa of a contact pressure at an approach speed of 1, 5, and 10 mm/s, respectively. In the SFP model, the fluid load support ratio was 68.7%, 70.3%, and 72.0% at 0.1 MPa of a contact pressure and 64.9%, 66.8%, and 67.4% at 0.26 MPa of a contact pressure at an approach speed of 1, 5, and 10 mm/s, respectively. The fluid load support ratio was slightly higher in the SFP model than that in the standard model at each approach speed of 1, 5 and 10 mm/s.

at 0.1 MPa of contact pressure (a) and 0.26 MPa of contact pressure (b).

4. Discussion

We performed an experimental and analytical study to determine the effect of fluid pressurization induced by the squeeze-film effect on the biphasic lubrication property of articular cartilage.

Two pressure peaks were observed in the temporal change of the fluid pressure in the fluid pressure measurement in contact area (Fig. 3a). Because the pressure induced by the squeeze-film effect was generated before contact, the first peak was defined as the highest squeeze-film pressure. The second peak of the measured pressure

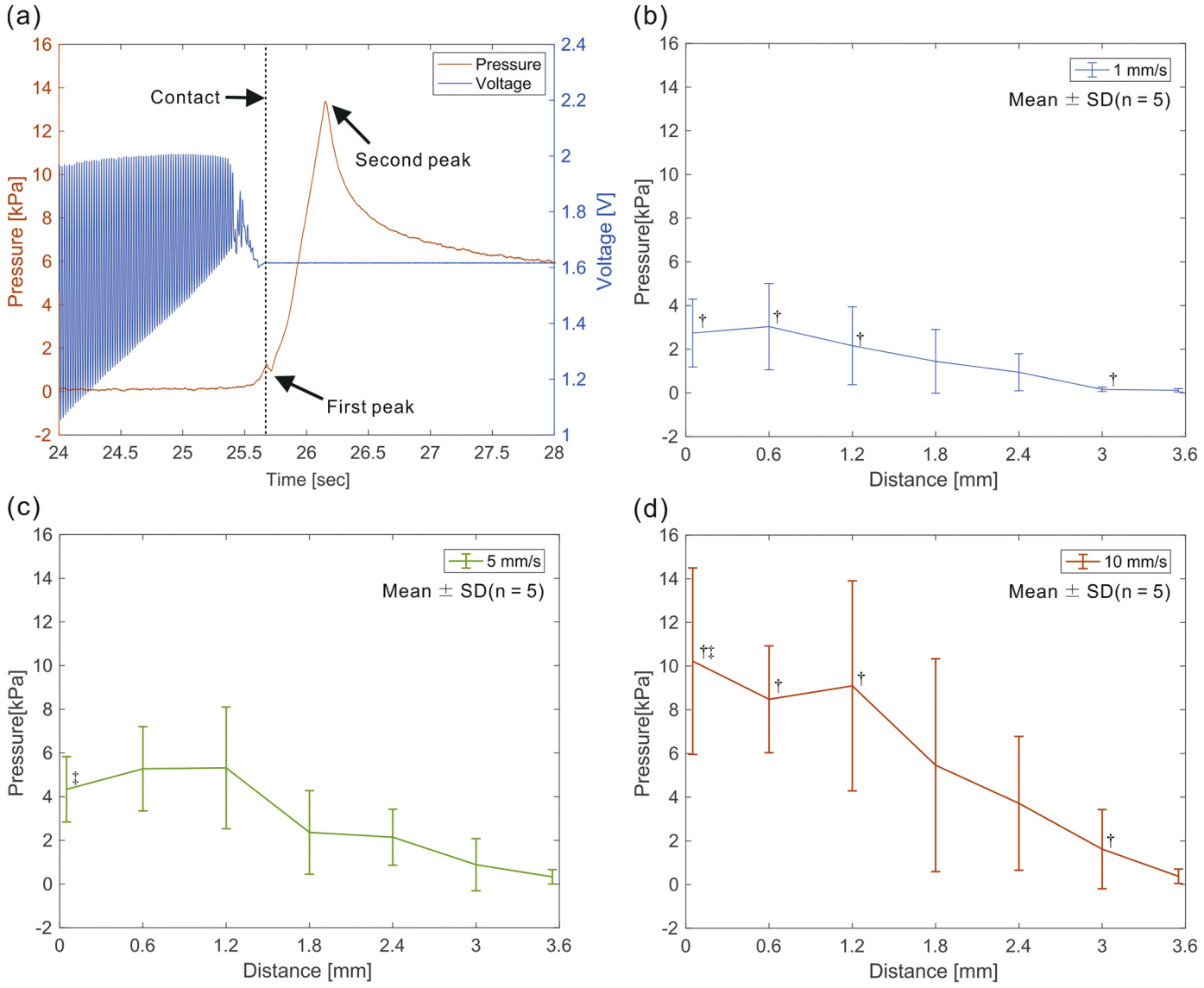

Fig. 3. Temporal change of the fluid pressure and voltage at an approach speed of 1 mm/s and at 1.0 mm from the center of the indenter (dotted line: moment of contact detected from voltage change) (a), Fluid pressure distribution at an approach speed of 1 mm/s (b), 5 mm/s (c), and 10 mm/s (d) by mean ± SD (n = 5, †: $p < .05$ (1 mm/s vs 10 mm/s), ‡: $p < .05$ (5 mm/s vs 10 mm/s) in Tukey-Kramer post hoc test), Distribution effect ($p < .05$), Speed effect ($p < .05$) in two-way mixed design ANOVA.

occurred owing to the penetration of polyurethane into the sensor hole after contact. To verify that the first peak was the highest squeeze-effect pressure, we repeated the experiment using the same method previously described with a stiffer indenter covered with polyacetal having a Young's modulus in the order of GPa. Therefore, only one peak of fluid pressure appeared at the time of contact. This result implied that the first pressure peak was caused by the squeeze-film effect. Moreover, the first peak pressure increased with an increasing approach speed (Fig. 3b–d). This tendency of that the fluid pressure increases due to increase in approach speed agreed with the natural behaviour of the fluid governed by hydrodynamic lubrication. Therefore, the first peak pressure was the highest pressure induced by the squeeze-film effect. However, the pressure peak at the centre as seen in the pressure distribution governed by squeeze-effect of hydrodynamic lubrication wasn't observed in the fluid pressure distribution results (Fig. 3b–d). As a result of measuring the surface shape of the indenter, the radius of curvature of the indenter surface was a bit larger than the assumed 15 mm and had the microscopic waviness. Therefore, it is considered that the surface shape of the indenter, especially within the contact region was not an ideal cylindrical shape but was flattened with the microscopic waviness due to the process of gluing polyurethane sheet onto the cylinder. This suggests that the fluid pressure distribution where there is no peak at the center and it has large variation in pressure due to the flattened shape of vertex areas of indenter with microscopic waviness. Ikeuchi et al. [31] and Ruggiero et al. [32] reported that high pressures in the order of MPa were generated by the squeeze motion in the hip joint and ankle joint, respectively. In biological joints, synovial fluid pressure may increase to a high value owing to the high conformity of the confronting articular cartilage surfaces. However, a contact model of a cylinder versus a plate was used for simplicity and generality of the experiment and analysis in this study. Because of the shape of the model and the limitation of the pressure measurement using the pin-hole, the measured fluid pressure could be lower in this study than that in a physiological situation. Moreover, the joint load may increase up to 2 kN within 0.2–0.4 s at the knee and hip joints in normal walking [33]. The approach speed set in this study was slower than that of physiological conditions. In addition, the viscosity of human synovial fluid reported by Cooke et al. [34] is in the order of

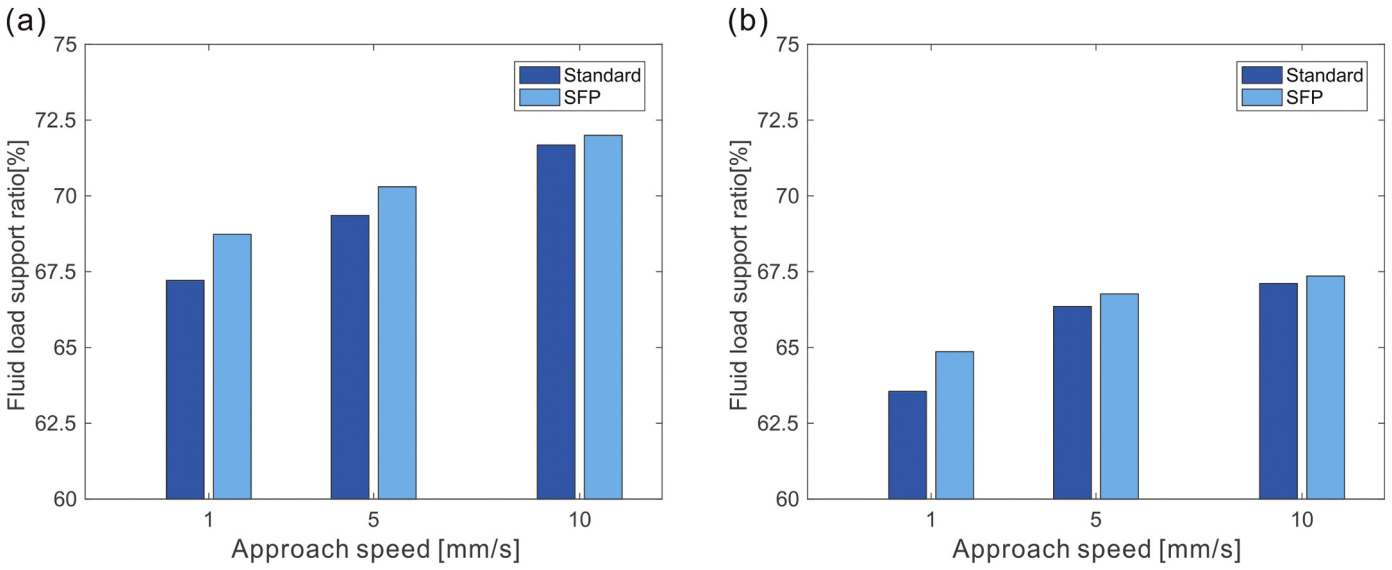

Fig. 4. Fluid load support ratio at the end of loading for each approach speed.

10^{-2} to 10^{2} Pa·s, while the viscosity of the lubricant used in this study was 10^{-1} Pa·s. This could be why the measured fluid pressure was low in this study. In addition, the elastic modulus and Poisson's ratio of polyurethane were used as mechanical properties of the cartilage model in order to make the analysis condition agree with that of the experiment. However, since the elastic modulus of articular cartilage is in the range of 0.2–1.3 MPa [3,35,36] and the Poisson's ratio is in the range of 0.42–0.50 [37–39], the values used in the analysis are within these cartilage mechanical properties. Therefore, the obtained information could be qualitative without providing numerical values; however, the information is valuable for evaluating the effect of fluid pressurization on the biphasic lubrication in articular cartilage.

The fluid load support ratio in the SFP model was higher than that of the standard model at each approach speeds of 1, 5 and 10 mm/s (Fig. 4). Because the contact force W was constant at loads of 0.1 MPa and 0.26 MPa, the fluid load support ratio was dependent on the integration of the pore pressure. The model of the fluid pressure outside of the cartilage suppressed the outflow of the interstitial fluid, which resulted in a pore pressure increase inside the cartilage in the SFP model. However, there was a slight effect of the fluid pressure when increasing the fluid load support ratio: 1.5%, 0.9% and 0.3% at 0.1 MPa of a contact pressure and 1.3%, 0.4%, and 0.2% at 0.26 MPa of a contact pressure at each approach speed of 1, 5 and 10 mm/s, respectively. Although the fluid pressure $p_w{}^{\infty}$ induced by the squeeze-film effect measured in this study was higher than that induced by the wedge-film effect reported in our previous study [24], the fluid load support showed a minimal increase in this study. The effect of the suppression of the interstitial fluid outflow by the synovial fluid pressure is controlled by a balance of two factors: the pore pressure p_w caused by deformation and the synovial fluid pressure $p_w{}^{\infty}$. Because the pore pressure p_w depends on the approach speed, the pore pressure exceeds the synovial fluid pressure $p_w{}^{\infty}$, and the fluid load support ratio was not affected by the synovial fluid pressure at an approach speed of 10 mm/s. In the compression analysis, the measured fluid pressure $p_w{}^{\infty}$ was applied to the gap between the cartilage model and rigid plate. The gap near the centre of the indenter disappeared at an early period of compression owing to the deformation of the indenter. Therefore, a higher fluid pressure near the centre of the indenter was applied for a short duration. This could have reduced the suppression effect of the fluid pressure as the contact pressure increased (Fig. 4). The differences in the fluid load support ratio between the SFP and standard models decreased with an increase of the load at each approach speed. Therefore, the effect of suppression was higher at a low load than that at a high load. The fluid pressurization induced by the squeeze-film effect could improve biphasic lubrication at an early stage of joint contact. Therefore, an experimental and analytical study of the entire articular motion, including the squeeze-film and wedge-film effects, should be performed.

In this study, a compression analysis was performed to determine the effect of the squeeze-film pressure, and a friction analysis was not performed. However, a higher fluid load support ratio at loading would contribute to the reduction of the friction coefficient immediately after the motion began. Because the squeeze-film effect thought to be the main regime of hydrodynamic lubrication as the lubrication mechanism of the cartilage [6,21], a high fluid pressure induced by the squeeze-film effect is expected to have a significant effect on biphasic lubrication. Further investigation is required to better understand the lubrication mechanism of articular cartilage.

5. Conclusion

We performed an experimental and analytical study on the effect of hydrodynamic fluid pressurization induced by the squeeze-film effect on the biphasic lubrication property of articular cartilage. The fluid load support increases owing to pressurization at the initial stage of contact; however, the overall effect was minimal for fluid pressurization induced by the squeeze-film effect using a simple contact model of a cylindrical-shaped elastic body against a rigid flat plate.

Acknowledgments

This study was supported by JSPS KAKENHI; Japan Society for the Promotion of Science(JSPS), Japan (grant-in-aid for scientific research (B), #16H03172) and Sasakawa Scientific Research Grant from the Japan Science Society, Japan. We would like to thank Editage (www.editage.jp) for English language editing.

References

[1] J. Charnley, The lubrication of animal joints in relation to surgical reconstruction by arthroplasty, Ann. Rheum. Dis. 19 (1960) 10–19, https://doi.org/10.1136/ard.19.1.10.
[2] T.A. Schmidt, R.L. Sah, Effect of synovial fluid on boundary lubrication of articular cartilage, Osteoarthr. Cartil. 15 (2007) 35–47, https://doi.org/10.1016/j.joca.2006.06.005.
[3] C.W. McCutchen, The frictional properties of animal joints, Wear 5 (1962) 1–17, https://doi.org/10.1016/0043-1648(62)90176-X.
[4] P.S. Walker, D. Dowson, M.D. Longfield, V. Wright, “Boosted lubrication” in

synovial joints by fluid entrapment and enrichment, Ann. Rheum. Dis. 27 (1968) 512–520, https://doi.org/10.1136/ard.27.6.512.
[5] D. Dowson, A. Unsworth, V. Wright, Analysis of boosted lubrication in human joints, J. Mech. Eng. Sci. 12 (1970) 364–369, https://doi.org/10.1243/JMES.
[6] D. Dowson, Paper 12: modes of lubrication in human joints, Proc. Inst. Mech. Eng. Conf. Proc. 181 (1966) 45–54, https://doi.org/10.1243/PIME_CONF_1966_181_206_02.
[7] G.A. Ateshian, H. Wang, W.M. Lai, The role of interstitial fluid pressurization and surface porosities on the boundary friction of articular cartilage, J. Tribol. 120 (1998) 241–248, https://doi.org/10.1115/1.2834416.
[8] G.A. Ateshian, The role of interstitial fluid pressurization in articular cartilage lubrication, J. Biomech. 42 (2009) 1163–1176, https://doi.org/10.1016/j.jbiomech.2009.04.040.
[9] V.C. Mow, S.C. Kuei, W.M. Lai, C.G. Armstrong, Biphasic creep and stress relaxation of articular cartilage in compression: theory and experiments, J. Biomech. Eng. 102 (1980) 73–84, https://doi.org/10.1115/1.3138202.
[10] M. Caligaris, G.A. Ateshian, Effects of sustained interstitial fluid pressurization under migrating contact area, and boundary lubrication by synovial fluid, on cartilage friction, Osteoarthr. Cartil. 16 (2008) 1220–1227, https://doi.org/10.1016/j.joca.2008.02.020.
[11] H. Fujie, K. Imade, Effects of low tangential permeability in the super fi cial layer on the frictional property of articular cartilage, Biosurface Biotribol. 1 (2015) 124–129, https://doi.org/10.1016/j.bsbt.2015.06.001.
[12] N. Sakai, Y. Hagihara, T. Furusawa, N. Hosoda, Y. Sawae, T. Murakami, Analysis of biphasic lubrication of articular cartilage loaded by cylindrical indenter, Tribol. Int. 46 (2012) 225–236, https://doi.org/10.1016/j.triboint.2011.03.016.
[13] N. Sakai, C. Hashimoto, S. Yarimitsu, Y. Sawae, M. Komori, T. Murakami, A functional effect of the superficial mechanical properties of articular cartilage as a load bearing system in a sliding condition, Biosurface Biotribol. 2 (2016) 26–39, https://doi.org/10.1016/j.bsbt.2016.02.004.
[14] S.S. Pawaskar, Z.M. Jin, J. Fisher, Modelling of fluid support inside articular cartilage during sliding, Proc. Inst. Mech. Eng. Part J J. Eng. Tribol. (2007) 165–174, https://doi.org/10.1243/13506501JET241.
[15] S. Graindorge, W. Ferrandez, Z. Jin, E. Ingham, C. Grant, P. Twigg, J. Fisher, Biphasic surface amorphous layer lubrication of articular cartilage, Med. Eng. Phys. 27 (2005) 836–844, https://doi.org/10.1016/j.medengphy.2005.05.001.
[16] J.S. Hou, V.C. Mow, W.M. Lai, M.H. Holmes, An analysis of the squeeze-film lubrication mechanism for articular cartilage, J. Biomech. 25 (1992) 247–259, https://doi.org/10.1016/0021-9290(92)90024-U.
[17] Z.M. Jin, D. Dowson, J. Fisher, The effect of porosity of articular cartilage on the lubrication of a normal human hip joint, Proc. Inst. Mech. Eng. Part H J. Eng. Med. 206 (1992) 117–124, https://doi.org/10.1243/PIME_PROC_1992_206_279_02.
[18] A.C. Moore, D.L. Burris, Tribological rehydration of cartilage and its potential role in preserving joint health, Osteoarthr. Cartil. 25 (2017) 99–107, https://doi.org/10.1016/j.joca.2016.09.018.
[19] B.T. Graham, A.C. Moore, D.L. Burris, C. Price, Sliding enhances fluid and solute transport into buried articular cartilage contacts, Osteoarthr. Cartil. 25 (2017) 2100–2107, https://doi.org/10.1016/j.joca.2017.08.014.
[20] B.T. Graham, A.C. Moore, D.L. Burris, C. Price, Mapping the spatiotemporal evolution of solute transport in articular cartilage explants reveals how cartilage recovers fluid within the contact area during sliding, J. Biomech. 71 (2018) 271–276, https://doi.org/10.1016/j.jbiomech.2018.01.041.
[21] R.S. Fein, Research report 3: are synovial joints squeeze-film lubricated? Proc. Inst. Mech. Eng. Conf. Proc. 181 (1966) 125–128, https://doi.org/10.1243/PIME_CONF_1966_181_215_02.
[22] S. Horibata, S. Yarimitsu, H. Fujie, Effect of synovial fluid pressure increase in a wedge-shaped gap on the biphasic lubrication property of articular cartilage, Jpn. J. Clin. Biomech. 39 (2017) 327–332 (in Japanese).
[23] S. Horibata, S. Yarimitsu, H. Fujie, Influence of synovial fluid pressure increase on the biphasic lubrication property of articular cartilage, Proc. Mech. Eng. Congr. Jpn. (2017) p. J0260104. in Japanese https://doi.org/10.1299/jsmemecj.2017.J0260104.
[24] S. Horibata, S. Yarimitsu, H. Fujie, Influence of synovial fluid pressure on biphasic lubrication property in articular cartilage, Tribol. Online 13 (2018) 172–177, https://doi.org/10.2474/trol.13.172.
[25] T. Murakami, H. Higaki, H. Ando, Y. Nakanishi, Viscous property of synovial fluids and related solutions and its role in joint lubrication, Trans. Jpn. Soc. Mech. Eng. Ser. C. 63 (1997) 750–756 in Japanese https://doi.org/10.1299/kikaic.63.750.
[26] M.F. Beatty, D.O. Stalnaker, The poisson function of finite elasticity, J. Appl. Mech. 53 (2009) 807, https://doi.org/10.1115/1.3171862.
[27] K. Imade, S. Mochizuki, T. Susa, R. Nansai, H. Fujie, Effects of interstitial fluid and boundary condition on the start-up friction behavior of cartilage, Proc. Int. Conf. Biotribol. (2012) 34.
[28] W.M. Lai, V.C. Mow, Drag-induced compression of articular cartilage during a permeation experiment, Biorheology 17 (1980) 111–123.
[29] N. Hashimoto, S. Yarimitsu, H. Fujie, Site and orientation dependencies of hydraulic permeability in immature articular carilage, Proc. 3rd Int. Conf. Biotribol. (2016) p. O5.01.
[30] T. Susa, J. Takeda, R. Nansai, N. Nakamura, H. Fujie, Finite element analysis of cartilage-like repaired tissure using a fiber-reinforced poroelastic model, Proc. 6th World Congr. Biomech. (2010) 428.
[31] K. Ikeuchi, M. Oka, H. Mori, A simulation of the squeeze film effect in a hip joint, Trans. Jpn. Soc. Mech. Eng. Ser. C. 55 (1989) 508–515 in Japanese https://doi.org/10.1299/kikaic.55.508.
[32] A. Ruggiero, E. Gòmez, R. D'Amato, Approximate analytical model for the squeeze-film lubrication of the human ankle joint with synovial fluid filtrated by articular cartilage, Tribol. Lett. 41 (2010) 337–343, https://doi.org/10.1007/s11249-010-9710-5.
[33] A. Unsworth, Tribology of human and artifical joints, Proc. Inst. Mech. Eng. 205 (1991) 1–10.
[34] A.F. Cooke, D. Dowson, V. Wright, The rheology of synovial fluid and some potential synthetic lubricants for degenerate synovial joints, Eng. Med. 7 (1978) 66–72, https://doi.org/10.1243/EMED_JOUR_1978_007_021_02.
[35] J.S. Jurvelin, M.D. Buschmann, E.B. Hunziker, Optical and mechanical determination of Poisson's ratio of adult bovine humeral articular cartilage, J. Biomech. 30 (1997) 235–241, https://doi.org/10.1016/S0021-9290(96)00133-9.
[36] C.C.B. Wang, N.O. Chahine, C.T. Hung, G.A. Ateshian, Optical determination of anisotropic material properties of bovine articular cartilage in compression, J. Biomech. 36 (2003) 339–353, https://doi.org/10.1016/S0021-9290(02)00417-7.
[37] W.C. Hayes, L.F. Mockros, Viscoelastic properties of human articular cartilage, J. Appl. Physiol. 31 (1971) 562–568, https://doi.org/10.1152/jappl.1971.31.4.562.
[38] G.E. Kempson, M.A.R. Freeman, S.A.V. Swanson, The determination of a creep modulus for articular cartilage from indentation tests on the human femoral head, J. Biomech. 4 (1971) 239–250, https://doi.org/10.1016/0021-9290(71)90030-3.
[39] R.Y. Hori, L.F. Mockros, Indentation tests of human articular cartilage, J. Biomech. 9 (1976) 259–268, https://doi.org/10.1016/0021-9290(76)90012-9.